

# Modelling of Nanoindentation of TiAlN and TiN Thin Film Coatings for Automotive Bearing



Wan Fathul Hakim W Zamri, Ng Jie Suang, Intan Fadhlina Mohamed, Ahmad Kamal Ariffin, Muhammad Faiz Md Din

**Abstract:** Bearings are critical components for the transmission of motion in machines. Automotive components, especially bearings, will wear out over a certain period of time because they are constantly subjected to high levels of stress and friction. Studies have proven that coatings can extend the lifespan of bearings. Hence, it is necessary to conduct studies on coatings for bearings, particularly the mechanical and wear properties of the coating material. This detailed study focused on the mechanical properties of single-coatings of TiN and TiAlN using the finite element method (FEM). The mechanical properties that can be obtained from nano-indentation experiments are confined to just the Young's modulus and hardness. Therefore, nanoindentation simulations were conducted together with the finite element method to obtain more comprehensive mechanical properties such as the yield strength and Poisson's ratio. In addition, various coating materials could be examined by means of these nanoindentation simulations, as well the effects of those parameters that could not be controlled experimentally, such as the geometry of the indenter and the bonding between the coating and the substrate. The simulations were carried out using the ANSYS Mechanical APDL software. The mechanical properties such as the Young's modulus, yield strength, Poisson's ratio and tangent modulus were 370 GPa, 19 GPa, 0.21 and 10 GPa, respectively for the TiAlN coating and 460 GPa, 14 GPa, 0.25 and 8 GPa, respectively for the TiN coating. The difference between the mechanical properties obtained from the simulations and experiments was less than 5 %.

**Keywords :** Automotive bearings, wear, Nanoindentation and Finite element method.

Manuscript published on 30 September 2019

\* Correspondence Author

**Wan Fathul Hakim W. Zamri**, Centre for Materials Engineering and Smart Manufacturing (MERCU), Faculty of Engineering and Built Environment, Universiti Kebangsaan Malaysia, Bangi, Malaysia. Email: wfathul.hakim@ukm.edu.my

**Ng JieSuang**, Centre for Materials Engineering and Smart Manufacturing (MERCU), Faculty of Engineering and Built Environment, Universiti Kebangsaan Malaysia, Bangi, Malaysia. Email: ngjiesuang94@gmail.com

**Intan Fadhlina Mohamed**, Centre for Materials Engineering and Smart Manufacturing (MERCU), Faculty of Engineering and Built Environment, Universiti Kebangsaan Malaysia, Bangi, Malaysia. Email: intanfadhlna@ukm.edu.my

**Ahmad kamal Ariffin**, Centre for Materials Engineering and Smart Manufacturing (MERCU), Faculty of Engineering and Built Environment, Universiti Kebangsaan Malaysia, Bangi, Malaysia. Email: kamal3@ukm.edu.my

**Muhammad Faiz Md Din**, Department of Electrical & Electronics, Faculty of Engineering, Universiti Pertahanan Nasional Malaysia, Kuala Lumpur, Malaysia. Email: kamal3@ukm.edu.my

© The Authors. Published by Blue Eyes Intelligence Engineering and Sciences Publication (BEIESP). This is an [open access](https://creativecommons.org/licenses/by-nc-nd/4.0/) article under the CC-BY-NC-ND license <http://creativecommons.org/licenses/by-nc-nd/4.0/>

## I. INTRODUCTION

Bearings are critical components for the transmission of motion in machines. Automotive components, especially bearings, will wear out over a certain period of time because they are constantly subjected to high levels of stress and friction. Therefore, automotive components need to be resistant to wear and friction in critical situations. As such, various types of coating materials have been introduced to overcome the problem of friction, which was causing the bearings to wear out. In tribology applications, coatings can harden and protect the surfaces of automotive components that are constantly shifting in critical situations.

Nanoindentation experiments were carried out to determine the mechanical properties of thin film coatings. However, the mechanical properties that were obtained through the nanoindentation experiments were confined to just the hardness and Young's modulus [21]. Therefore, for those mechanical properties that are difficult to determine experimentally, such as the yield strength and Poisson's ratio, nanoindentation simulations with the finite element method (FEM) were conducted. In addition, the nano-indentation simulations could be used to study various parameters without incurring any costs, which otherwise could not be controlled in experiments, such as the effects of the substrate, the geometry of the indenter, the friction between the indenter tip and the surface of the coated specimens [3], [8], [11].

This study was aimed at investigating the mechanical properties of monolithic (single) coatings using nanoindentation simulations by the finite element method. The simulation results were validated by comparing them with the experimental results obtained by [11] and [18].

## II. MATERIAL & MODELLING PROCEDURES

Figure 1 shows the workflow for the entire study. The ANSYS Mechanical APDL R16.0 software was used for the nano-indentation simulations. The validation of the precision of the model by the finite element method was done by comparing the modelling results with the data from the nano-indentation experiments performed by [18] and [11]. The data from the nanoindentation experiments that were used as the basis for the comparison were the load-displacement curves.

At the start, the type of element was modelled using PLANE 182, which had four nodes with two degrees of freedom at each node. The PLANE 182 is suitable for models with solid structures.

The convex tip of the indenter, which had the same properties as a Berkovich indenter with an included angle of  $70.3^\circ$ , was used in the FEM simulation. As the indenter was made of diamond, which does not undergo any plastic deformation, it was modelled as a rigid or perfectly inelastic material. The coating materials were modelled as elastic with linear strain hardening (bi-linear material models). The HSS (High speed steel) substrate was modelled as a perfectly plastic material since no plastic deformation occurred at the substrate. It was assumed that the coating and substrate were homogeneous and isotropic materials.

The contact between the 2-D (TARGE 169) target surfaces was modelled using the CONTA 171. In this case, the coating surface represented a deformable contact surface, while the target surface represented the surface of the indenter tip. For the boundary conditions, all the nodes on the Y-axis could only move towards Y and all the nodes on the X-axis were fixed and immovable. The base of the indenter had a fixed and restricted boundary. When the base of the substrate was displaced, the coating moved together with the substrate to be finally penetrated by the indenter tip. Furthermore, it was assumed that there was no residual stress in the coating and the substrate following the deposition process. The contact was perfect and it was assumed that there was no friction between the indenter tip and the coating. A high degree of meshing was applied to the point of contact between the indenter tip and the coating. Figure 2 shows the boundary conditions of the model.

Next, iterative inputs for the Young's modulus ( $E$ ), Poisson's ratio ( $\nu$ ), yield strength  $\sigma_y$ , and tangent modulus ( $E_T$ ) were carried out to obtain the equivalent load-displacement curves to those that had been obtained experimentally. The mechanical properties of the coatings could be determined if the gradient of the unloading curve

$$S = \frac{dP}{dh}$$

were less than 10% compared to the experimental load-displacement curves. The nano-indentation simulations were divided into two parts, the loading and unloading. The nano-indentation loading was simulated with a lower displacement towards Y until the coated specimen came into contact with and was penetrated by the indenter tip to achieve the maximum depth of indentation. Meanwhile, the unloading process occurred with the coated specimen returning to its original position. The maximum depth of indentation had to be less than 10% of the thickness of the coating to avoid any impact on the substrate [7].

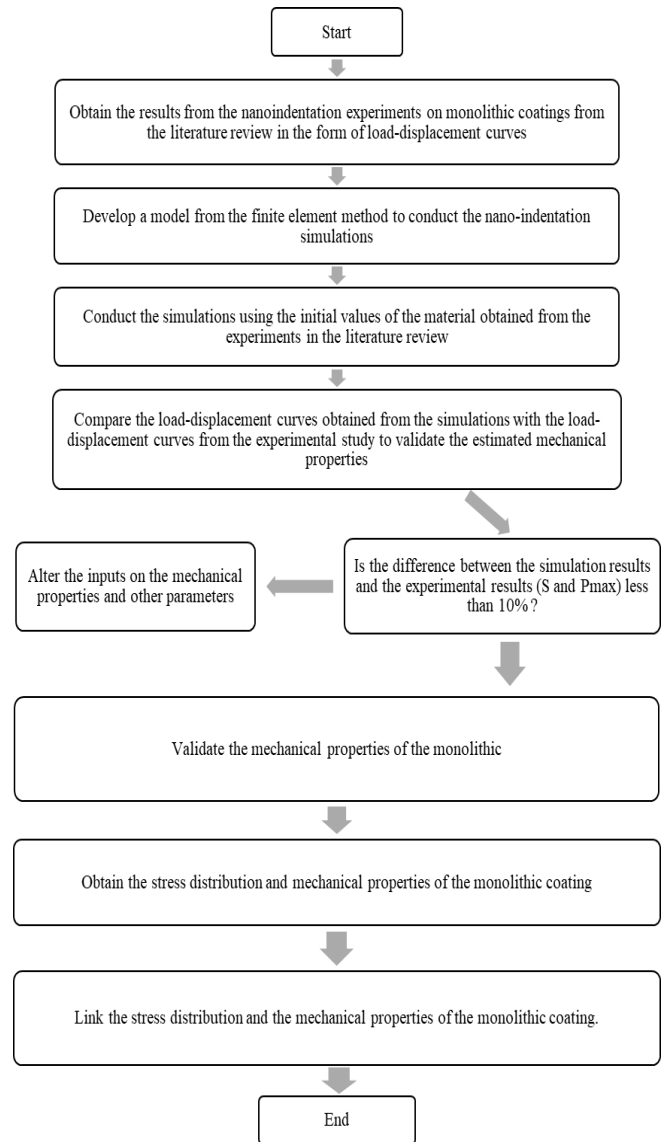


Fig. 1. Workflow of the entire study.

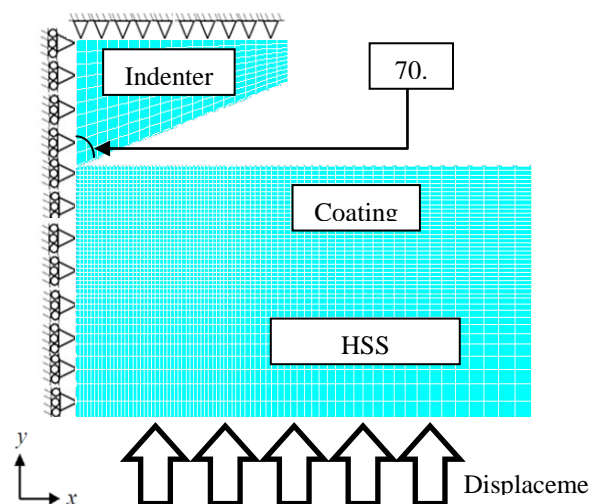
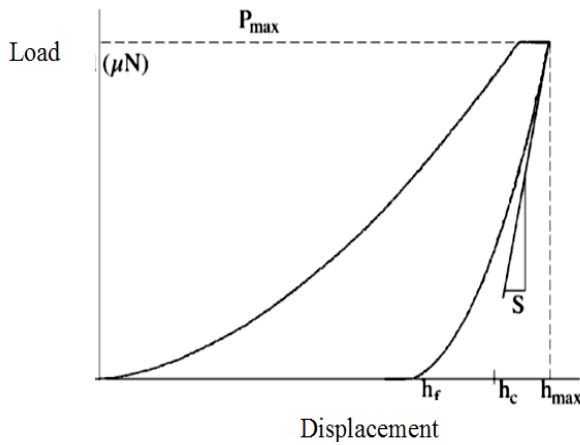


Fig. 2. Model of boundary conditions.

**A. Formula for the calculation of the nanoindentation load-displacement curve**

Figure 3 shows an example of the load-displacement curve with maximum load,  $P_{max}$ , maximum depth of indentation,  $h_{max}$ , and empty load indentation depth,  $h_f$ .



**Fig. 3. Load-displacement curve.**

The hardness,  $H$  was calculated using equations (1), (2) and (3).

$$H = \frac{P_{max}}{A_c} \tag{1}$$

$$A_c = 24.5h_c^2 \tag{2}$$

$$h_c = h_{max} - \epsilon(h_{max} - h_f) \tag{3}$$

where  $A_c$  is the area of contact between the indenter tip and the material being tested, and  $h_c$  is the depth of the point of contact. The intercept factor,  $\epsilon$  of the convex indenter was 0.72 for the indenter and 0.75 for the Berkovich indenter [16].

In this study, the formula that was used to calculate the hardness,  $H$  improved the speed of the calculation and the accuracy of the answer, as reported by [20] and [8] compared to the method of drawing lines at the unloading curve.

**III. RESULT AND DISCUSSION**

The load-displacement curves for the TiAlN and TiN coating experiment and simulation are shown in Figure 4 and Figure 5, respectively. The results for the TiAlN nano-indentation experiment were taken from the latest nanoindentation study by Swain et al. (2017), while the results for the TiN nanoindentation experiment were taken from [11]. Both simulations gave good results which were almost similar to the experimental results. The differences in the unloading

gradient (unloading curve)  $S = \frac{dP}{dh}$  and the maximum load

$P_{max}$  for the experiments and the simulations were less than 10%.

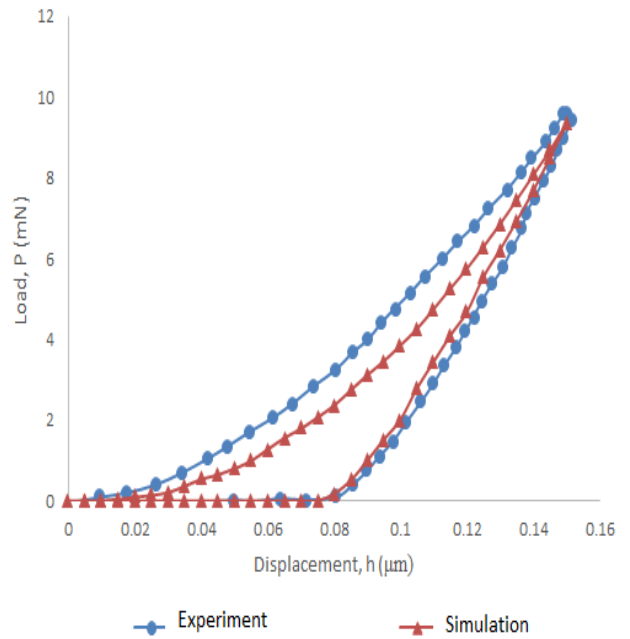


**Fig. 4. Load-displacement curves for monolithic TiAlN coating experiment and simulation.**

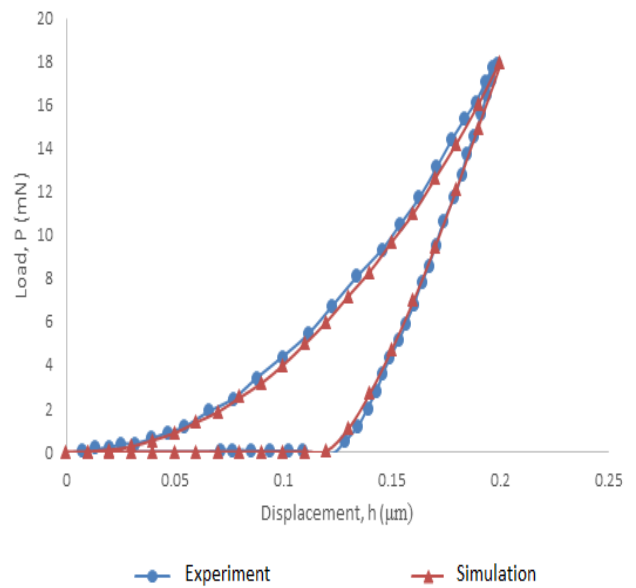


**Fig. 5. Load-displacement curves for monolithic TiN coating experiment and simulation.**

Table I and Table II show the comparison of the mechanical properties of TiAlN and TiN, respectively that were obtained through nanoindentation simulations with the mechanical properties cited from a literature review of such experiments.

Based on Table I, the Young's modulus for the TiAlN coating was in the range of 30 GPa to 38 GPa. The hardness for the TiAlN coating, according to the current simulation results, was 38.39 GPa, which was 12.81 % higher than the average of all the hardness values in the literature review.

For the Young’s modulus, the current simulation result was 7 % lower than the average of the Young’s modulus taken from the literature review. On the other hand, the hardness of the TiN coating was in the range of 21 GPa to 37 GPa. The hardness of the TiN coating according to the current simulation result was 36.07 GPa, which was 21.65 % higher than the average result of the literature review so far. The relatively high difference for the TiN coating was because all the studies in the literature review to date did not have very

consistent values for the TiN coating. For the Young’s modulus, the current simulation result was 7.05 % higher than the average result from the literature review. All these differences in values can be attributed to the residual stress, roughness of the coating surface and the geometry of the indenter (Fischer-Cripps, 2002). In addition, more comprehensive mechanical properties could be obtained by using the finite element method of simulation compared to the nanoindentation experiment.

**Table- I: Comparison of mechanical properties from a literature review of experiments with the current simulation of a TiAlN monolithic coating**

Hardness, $H$ (GPa)	Young’s Modulus, $E$ (GPa)	Poisson’s Ratio, $\nu$	Yield Strength, $\sigma_y$ (GPa)	Tangent Modulus, $E_T$ (GPa)	Reference
38.39	370	0.21	19	10	Current simulation results
36.2	-	-	-	-	[10]
37.4	460	-	-	-	[24]
32.02	350	-	-	-	[4]
30	-	-	-	-	[17]
36.1	459	-	-	-	[25]
35	388	-	-	-	[13]
38	-	-	-	-	[18]
30.7	-	-	-	-	[5]
30	-	-	-	-	[12]
31.4	322.2	-	-	-	[15]
33.8	-	-	-	-	[14]

**Table- II: Comparison of mechanical properties from literature review of experiments with the current simulation of a TiN monolithic coating**

Hardness, $H$ (GPa)	Young’s Modulus, $E$ (GPa)	Poisson’s Ratio, $\nu$	Yield Strength, $\sigma_y$ (GPa)	Tangent Modulus, $E_T$ (GPa)	Reference
36.07	460	0.25	14	8	Current simulation results
37	450	0.25	14.5	-	[11]
35	-	-	-	-	[2]
21	300	0.25	-	-	[9]
-	300	0.25	-	-	[26]
24	-	-	-	-	[12]
-	400	0.25	-	-	[19]
33.6	447	0.21	-	-	[6]
27.3	351.3	-	13.83	-	[1]

Figure 6 shows the von Mises stress distribution for the TiAlN and TiN coatings during maximum loading. The maximum stress occurred at the point of contact between the coating surface and the indenter tip. The maximum depth of indentation for the TiAlN and TiN coatings was less than 10% of the thickness of the coating. This was so in order to reduce any impact on the substrate. According to Figure 6, no von Mises stress contours were applied to the HSS substrate. The stress contours for the TiAlN and TiN coatings were circular in shape and spread out smoothly from the point of contact between the surface and the indenter tip. The TiAlN coating experienced a higher von Mises stress of 39.348 GPa

compared to the TiN coating, which was 31.48 GPa. In other words, TiAlN has a higher hardness because the TiAlN coating required a greater stress to be indented to a specified depth during the loading process.

Figure 7 shows the equivalent plastic strain distribution for the TiAlN and TiN coatings during the full unloading. The plastic strain, which is also known as the plastic deformation, occurred at the point of contact between the coating surface and the indenter tip.

Furthermore, a few plastic strain contours spread smoothly from the point of contact between the surface and the indenter tip, and these had no effect on the equivalent plastic strain contours to the HSS substrate. This was important to prevent any impact on the substrate and to accurately obtain the mechanical properties of the coatings. The maximum equivalent plastic strain for the TiAlN coating was 0.472701,

while the maximum equivalent plastic strain for the TiN coating was 0.679421. The TiAlN and TiN coatings experienced plastic strain because the von Mises stress experienced by the coatings exceeded their yield strength and indirectly contributed to the plastic deformation of the coatings, whereby the coatings would never fully return to their original shape (Silicon As 1982) [22], [23].

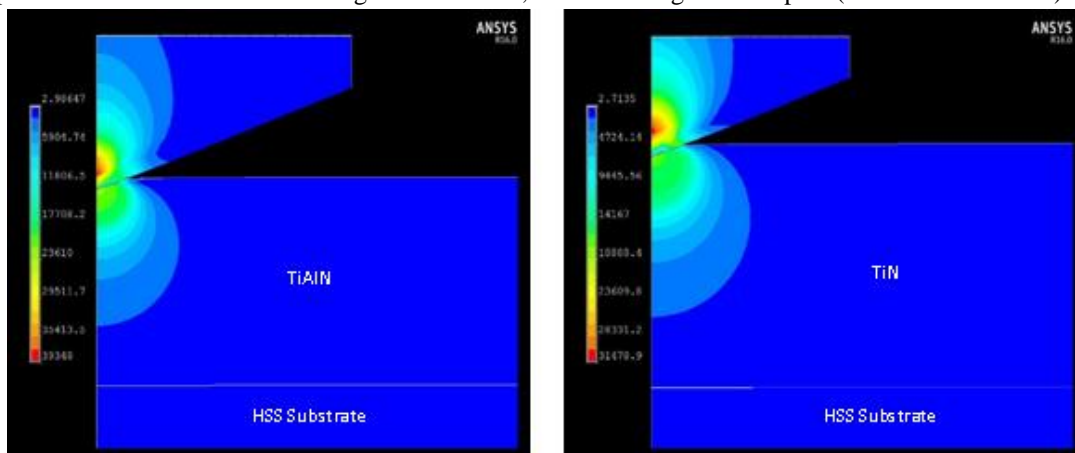


Fig. 6. Von Mises stress distribution for TiAlN and TiN coatings during maximum loading (stress unit in MPa)

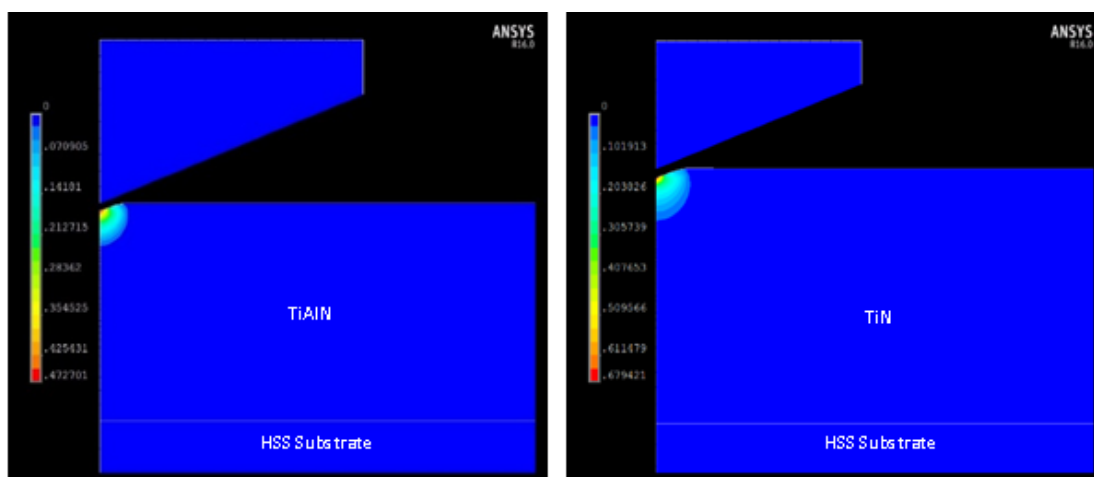


Fig. 7. Equivalent plastic strain distribution for TiAlN and TiN coatings during full unloading.

#### IV. CONCLUSION

The advantage of using the nanoindentation simulation was that it was able to provide those mechanical properties that are difficult to obtain through experiments such as the yield strength and Poisson’s ratio. The mechanical properties of the TiAlN coating, such as the Young’s modulus, yield strength, Poisson’s ratio and tangent modulus were 370 GPa, 19 GPa, 0.21 and 10 GPa, respectively, while for the TiN coating they were 460 GPa, 14 GPa, 0.25, 8 GPa, respectively. The difference in the mechanical properties between the simulation and experimental results was less than 5 %. In addition, the nanoindentation simulations were able to provide the stress contours and the stress that was experienced by the coatings. Apart from not incurring high costs, the nano-indentation simulations were able to alter the experimental perimeters such as the geometry of the indenter, the depth of the indentation, the thickness of the coating and so on.

#### V. ACKNOWLEDGEMENT

The authors would like to thank the Malaysia research foundation - Geran Universiti Penyelidikan: GUP-2018-149: for funding this work. This project also has received funding from the European Unions’s Horizon 2020 research and innovation programme under the Marie Skłodowska-Curie grant agreement No 730888.

#### REFERENCES

1. An, J. and Zhang, Q.Y., 2005. Structure, morphology and nanoindentation behavior of multilayered TiN/TaN coatings. *Surface and Coatings Technology*, 200(7), pp.2451-2458.
2. Bhowmick, S., Jayaram, V. and Biswas, S.K., 2005. Deconvolution of fracture properties of TiN films on steels from nanoindentation load–displacement curves. *Acta materialia*, 53(8), pp.2459-2467.

3. Bolshakov, A., Oliver, W.C. and Pharr, G.M., 1994. An explanation for the shape of nanoindentation unloading curves based on finite element simulation. *MRS Online Proceedings Library Archive*, 356.
4. Çalıřkan, H. and Küçükköse, M., 2015. The effect of aCN/TiAlN coating on tool wear, cutting force, surface finish and chip morphology in face milling of Ti6Al4V superalloy. *International Journal of Refractory Metals and Hard Materials*, 50, pp.304-312.
5. Chen, L., Pei, Z., Xiao, J., Gong, J. and Sun, C., 2017. TiAlN/Cu nanocomposite coatings deposited by filtered cathodic arc ion plating. *Journal of Materials Science & Technology*, 33(1), pp.111-116.
6. Chou, W.J., Yu, G.P. and Huang, J.H., 2002. Mechanical properties of TiN thin film coatings on 304 stainless steel substrates. *Surface and Coatings Technology*, 149(1), pp.7-13.
7. Huang, X. and Pelegri, A.A., 2007. Finite element analysis on nanoindentation with friction contact at the film/substrate interface. *Composites science and technology*, 67(7-8), pp.1311-1319.
8. Karimzadeh, A., Ayatollahi, M.R. and Alizadeh, M., 2014. Finite element simulation of nano-indentation experiment on aluminum 1100. *Computational Materials Science*, 81, pp.595-600.
9. Kumar, M. and Mitra, R., 2017. Effect of substrate temperature and annealing on structure, stress and properties of reactively co-sputtered Ni-TiN nanocomposite thin films. *Thin Solid Films*, 624, pp.70-82.
10. Li, D., Chen, J., Zou, C., Ma, J., Li, P. and Li, Y., 2014. Effects of Al concentrations on the microstructure and mechanical properties of Ti-Al-N films deposited by RF-ICPIS enhanced magnetron sputtering. *Journal of Alloys and Compounds*, 609, pp.239-243.
11. Lichinchi, M., Lenardi, C., Haupt, J. and Vitali, R., 1998. Simulation of Berkovich nanoindentation experiments on thin films using finite element method. *Thin solid films*, 312(1-2), pp.240-248.
12. Ma, L.W., Cairney, J.M., Hoffman, M.J. and Munroe, P.R., 2006. Deformation and fracture of TiN and TiAlN coatings on a steel substrate during nanoindentation. *Surface and Coatings Technology*, 200(11), pp.3518-3526.
13. Riedl, H., Koller, C.M., Munnik, F., Hutter, H., Martin, F.M., Rachbauer, R., Kolozsvari, S., Bartosik, M. and Mayrhofer, P.H., 2016. Influence of oxygen impurities on growth morphology, structure and mechanical properties of Ti-Al-N thin films. *Thin Solid Films*, 603, pp.39-49.
14. Santana, A.E., Karimi, A., Derflinger, V.H. and Schütze, A., 2005. Relating hardness-curve shapes with deformation mechanisms in TiAlN thin films enduring indentation. *Materials Science and Engineering: A*, 406(1-2), pp.11-18.
15. Shum, P.W., Zhou, Z.F., Li, K.Y. and Shen, Y.G., 2003. XPS, AFM and nanoindentation studies of Ti<sub>1-x</sub>Al<sub>x</sub>N films synthesized by reactive unbalanced magnetron sputtering. *Materials Science and Engineering: B*, 100(2), pp.204-213.
16. Sneddon, I.N., 1965. The relation between load and penetration in the axisymmetric Boussinesq problem for a punch of arbitrary profile. *International journal of engineering science*, 3(1), pp.47-57.
17. Sprute, T., Tillmann, W., Grisales, D., Selvadurai, U. and Fischer, G., 2014. Influence of substrate pre-treatments on residual stresses and tribo-mechanical properties of TiAlN-based PVD coatings. *Surface and Coatings Technology*, 260, pp.369-379.
18. Swain, N., Venkatesh, V., Kumar, P., Srinivas, G., Ravishankar, S. and Barshilia, H.C., 2017. An experimental investigation on the machining characteristics of Nimonic 75 using uncoated and TiAlN coated tungsten carbide micro-end mills. *CIRP Journal of Manufacturing Science and Technology*, 16, pp.34-42.
19. Tekaya, A., Benameur, T., Labdi, S. and Aubert, P., 2013. Effect of Ti/TiN multilayer protective nanocoatings on Zr-based metallic glasses mechanical performance. *Thin Solid Films*, 539, pp.215-221.
20. Wagih, A. and Fathy, A., 2016. Experimental investigation and FE simulation of nano-indentation on Al-Al<sub>2</sub>O<sub>3</sub> nanocomposites. *Advanced Powder Technology*, 27(2), pp.403-410.
21. Zamri, W.F.H., Kosasih, P.B., Tieu, A.K., Zhu, H. and Zhu, Q., 2013. Finite element modeling of the nanoindentation of layers of porous oxide on high speed steel. *steel research international*, 84(12), pp.1309-1319.
22. Zamri, W.F.H.W., Kosasih, B., Tieu, K., Ghopa, W.A.W., Din, M.F.M., Aziz, A.M. and Hassan, S.F., 2016. A simulation of friction behavior on oxidised high speed steel (HSS) work rolls. *ARPN Journal of Engineering and Applied Sciences*, 11(12), pp.7394-7400.
23. Zamri, W.F.H.W., Kosasih, B., Tieu, K., Ghopa, W.A.W., Din, M.F.M., Aziz, A.M. and Hassan, S.F., 2015. Effect of Carbide Particles on the Behaviour of the Oxide Layer. *Research Journal of Applied Sciences, Engineering and Technology*, 11(8), pp.910-920.
24. Zhang, K., Deng, J., Meng, R., Lei, S. and Yu, X., 2016. Influence of laser substrate pretreatment on anti-adhesive wear properties of WC/Co-based TiAlN coatings against AISI 316 stainless steel.

*International Journal of Refractory Metals and Hard Materials*, 57, pp.101-114.

25. Zhang, K., Deng, J., Sun, J., Jiang, C., Liu, Y. and Chen, S., 2015. Effect of micro/nano-scale textures on anti-adhesive wear properties of WC/Co-based TiAlN coated tools in AISI 316 austenitic stainless steel cutting. *Applied Surface Science*, 355, pp.602-614.
26. Zhao, X., Xie, Z. and Munroe, P., 2011. Nanoindentation of hard multilayer coatings: Finite element modelling. *Materials Science and Engineering: A*, 528(3), pp.1111-1116.

## AUTHORS PROFILE



**Wan Fathul Hakim Bin Wan Zamri** is a senior lecturer at Universiti Kebangsaan Malaysia (UKM). He obtained his bachelor at Universiti Kebangsaan Malaysia (UKM) and PhD at University of Wollongong, Australia. His expertise are computational tribology and wear of materials.



**Ng Jie Suang** is an undergraduate Mechanical Engineering student at Universiti Kebangsaan Malaysia (UKM). His Final Year Project (FYP) is under the supervision of Dr Wan Fathul Hakim Bin Wan Zamri.



**Intan Fadhlina Binti Mohamed** is a senior lecturer at Universiti Kebangsaan Malaysia (UKM). She obtained her bachelor and master at Universiti Kebangsaan Malaysia while PhD at KYUSHU University. Her expertise are severe plastic deformation, nanostructured materials and precipitation hardening.



**Ahmad kamal Ariffin Bin Mohd Ihsan** is a professor at Universiti Kebangsaan Malaysia (UKM). He obtained his bachelor at Universiti Kebangsaan Malaysia (UKM) and PhD at University of Wales. His expertise are computational methods, fracture mechanics, friction, corrosion, finite element/discrete element and parallels computations.



**Muhammad Faix Md Din** is a lecturer at Universiti Pertahanan Nasional Malaysia. He obtained his bachelor and master at University of Huddersfield while PhD at University of Wollongong, Australia. His expertise are superconductor, semiconductor, magnetism material, condenser matter, advance material application, renewable energy, magnetocaloric effect, X-ray diffraction and neutron diffraction.